# Green Emission in Ladder-Type Quarterphenyl: Beyond the Fluorenone-Defect

*Björn Kobin, Francesco Bianchi, Simon Halm, Joachim Leistner, Sylke Blumstengel, Fritz Henneberger,* and Stefan Hecht**

**In polyfluorenes it is generally accepted that (photo)degradation leads to fluorenone type defects that accept the excitation energy and emit green-to-yellow light with rather low efficiency. Although initial spectroscopic studies suggest the same to hold true for ladder-type poly(*para*-phenylene)s (LPPPs), kinetic studies of the degradation process are not compatible with the established mechanism. In general, the observed green emission can be caused by the introduction of carbonyl groups; however, only if associated with an additional disruption of the backbone rigidity and hence planarity of the entire $\pi$-system. This is clearly shown by comparison with synthesized model compounds, which are bearing the fluorenone motif yet possess very different optical properties as compared to the defects, which are actually formed. Degradation can be caused by solvent specific, yet substrate nonspecific aromatic formylation but mainly originates from reaction with in-situ generated singlet oxygen, both in solution as well as in thin films. Time-dependent photoluminescence measurements on thin films show that green emission is enhanced by energy transfer from intact molecules to defect centers.**

## 1. Introduction

In the past years there has been a lot of research in the field of organic electronics with the prospect of fabricating low-cost, light-weight, and flexible devices.[1] However, in organic photovoltaics (OPV) and in organic light-emitting diodes (OLED), especially the blue emitting ones, the lifetimes of the devices remains a critical issue. Polyfluorenes, as well as ladder-type poly(*para*-phenylene)s (LPPPs)[2] have already been exploited in blue emitting OLEDs for some time,[3] but they suffer from relatively fast degradation. There are several studies on the degradation of such compounds. The degradation can be initiated thermally, photochemically or electrochemically. In polyfluorenes (PF) the emerging green emission has been attributed to excimers and fluorenone defects, which are capable of trapping the excitation energy.[4] Furthermore chain end defects, such as hydroxyl groups, which originate from Suzuki cross couling polymerization, may lead to green emission as well.[5] In LPPPs a break of the bridging units of the polymer backbone was taken into consideration, as well as fragments, such as aryl ketones and fluorenones were identified by vibrational spectroscopy.[6,7] The optical properties of these fragments have also been characterized by means of quantum-chemical calculations and compared to the properties of thermally degraded LPPP films.[7] The most prominent mechanisms of degradation proposed in the literature involve a 9-fluorenylhydroperoxide formed from synthetic defect sites, such as residual 9-hydrogen-substituted fluorene.[4a] In addition, free-radical autoxidation leading to fluorenone type defects has been proposed for thermally[8] as well as photochemically[9] induced degradation, typically necessitating synthetic defect-sites. There is also at least one report on highly purified oligo(alkylfluorene)s, which alternatively claims that gradual degradation of the side chains due to singlet oxygen leads to the fluorenone defect.[10]

In contrast to most of these studies dealing with PF, we focus on small molecules, such as the ladder-type quarterphenyl **L4P**, which in combination with ZnO is supposed to be a potent candidate for creating hybrid inorganic-organic systems for opto-electronic devices.[11] In order to assemble these systems, **L4P** was designed to be compatible with organic molecular vapor-deposition, and therefore the molecular weight was minimized by limiting the number of repeat units and omitting solubilizing side chains. In this context it should be emphasized that the small-molecule approach—after proper purification by gradient-sublimation and crystallization—provides a pure sample compound of one well-defined molecular entity, which can be unambiguously structurally characterized. Here, we present a detailed study of the photodegradation of **L4P**, with detailed insights into its kinetics in solution as well as the chemical structure of formed degradation products. Particular attention is on the active species of oxygen being responsible for degradation. The optical properties of the isolated structural defects, deliberately synthesized fluorenone-type defects, and crude degraded mixtures are being compared, showing that

B. Kobin, Dr. J. Leistner, Prof. S. Hecht
Department of Chemistry and IRIS Adlershof
Humboldt-Universität zu Berlin
Brook-Taylor-Str. 2 12489, Berlin, Germany
E-mail: sh@chemie.hu-berlin.de

F. Bianchi, Dr. S. Halm, Dr. S. Blumstengel, Prof. F. Henneberger
Institut für Physik and IRIS Adlershof
Humboldt-Universität zu Berlin
Newtonstr. 15 12489, Berlin, Germany
E-mail: fh@physik.hu-berlin.de

**DOI: 10.1002/adfm.201402638**

the observed absorption and emission characteristics of the degraded samples cannot be explained by the conventional fluorenone-type defect in LPPPs. Finally, time-dependent photoluminescence (PL) measurements show that intact **L4P** is efficiently transferring its excitation energy to defects.

## 2. Synthesis

The synthesis of the two ketones **L4P-O** and **L4P-O2**[12] involves in both cases cross-coupling of properly substituted phenyl residues to a central fluorene building block (**Scheme 1**). In the first case of **L4P-O**, annulation proceeds by twofold Friedel-Crafts alkylation of the protected fluorenone core. On the other hand, twofold Friedel-Crafts acylation of a central fluorene building block creates the two terminal ketone functionalities in **L4P-O2**. Recently, we also published a synthesis yielding **L4P**,[11d,12] which has been designed to prepare longer oligomers and therefore involves many reaction steps. Comparing the different syntheses, we recommend the route via diester **10** described herein for facile access of **L4P**.

For the synthesis of **L4P-O** (Scheme 1a), 2,7-dibromofluorenone **2** was chosen as the central building block as well as 2-(methoxymethyl)-bromobenzene as the outer building block carrying the masked groups for intramolecular cyclization. Ether **1** was synthesized from 2-bromobenzyl bromide and sodium methoxide. The synthesis of 2,7-dibromofluorenone was adapted from an old, yet simple protocol by Goldschmiedt and Schranzhofer.[13] Ether **1** was converted to a boronic ester via lithiation and coupled twice to **2** via Suzuki crosscoupling using conditions, which were adapted from a paper by Knochel involving $Pd(dppf)Cl_2$ as catalyst and $Cs_2CO_3$ as base.[14] Oxidation of diether **3** with $KMnO_4$ yielded diester **4** in good yield.[15] Then, the ketone was protected as its dimethyl ketal using trimethyl orthoformate and toluenesulfonic acid. Subsequently, the ester-functionalities of **5** were reacted with methyl lithium to yield a tertiary alcohol intermediate, which was not isolated. For the twofold condensation to the desired ring-closed product, a Lewis acid needs to be employed, which – if used alone – was found to deprotect the ketone and eliminate the tertiary alcohols,

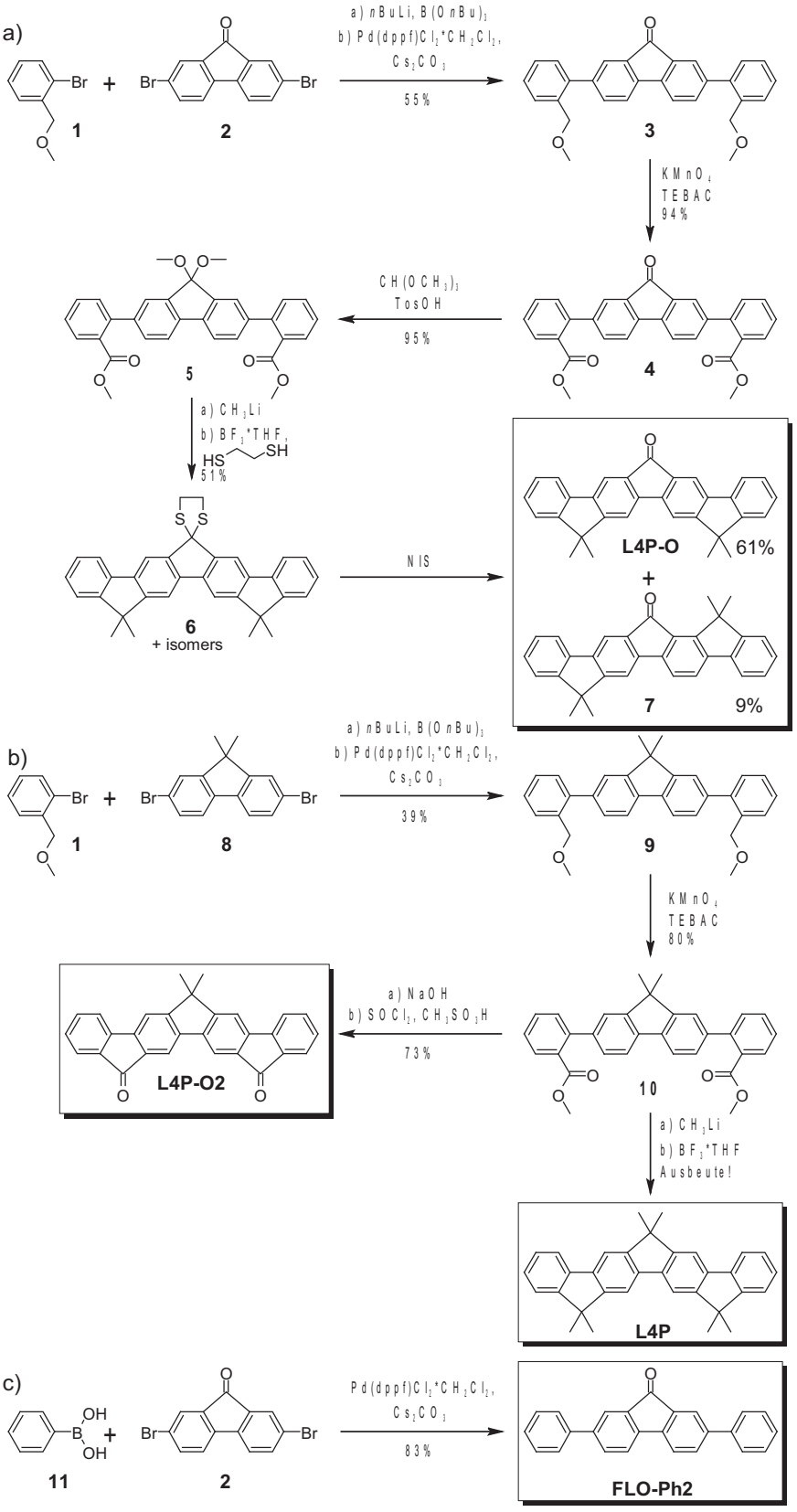


**Scheme 1.** Investigated fluorene and fluorenone derivatives and their synthesis: a) Synthesis of **L4P-O**, b) synthesis of **L4P-O2** and **L4P**, and c) synthesis of **FLO-Ph2**.

followed by further decompostion. In contrast, addition of 1,2-ethanedithiol (in the presence of the Lewis acid) led to conversion of the ketone to 1,3-dithiolane **6**, which is stable in the presence of the Lewis acid, as well as a minor amount of isomers (that have not been separated). Deprotection with N-iodosuccinimide and acetic acid gave the desired **L4P-O** as the main product as well as traces of **7**, which can easily be separated by column chromatography or crystallization.

The synthesis of **L4P-O2** (Scheme 1b) is rather straightforward: Ether **1** was coupled to 2,7-dibromofluorene **8** to yield diether **9**, which was subsequently oxidized to the diester **10** and hydrolyzed to the free acid. Condensation to **L4P-O2** was achieved by reaction of the bisacid with thionyl chloride and methanesulfonic acid as catalyst. Depending on the purity and morphology, **L4P-O2** appears as orange powder or deep orange to reddish crystals.

The semi-bridged **FLO-Ph2** was obtained by coupling phenylboronic acid **11** and 2,7-dibromofluorenone **2** (Scheme 1c). During this reaction only few amounts of side-products were formed and hence **FLO-Ph2** could be crystallized from the crude product in good yields.

## 3. Photodegradation in Solution

To investigate the chemical reactions, which give rise to photodegradation of samples containing **L4P**, some initial experiments were carried out in solution. In contrast to thin films it is relatively simple to keep the samples homogenous and hence the experimental conditions are defined more precisely while at the same time chemical analysis is facilitated. In an initial set of experiments, the influence of different solvents on the process of photodegradation was analyzed by exposing the respective solutions to strong UV-irradiation while acquiring photoluminescence (PL) spectra (see Supporting Information: Figure S5.1). Photodegradation is strongly dependent on the solvent, for example in toluene and tetrahydrofuran (THF) it is relatively slow whereas solutions in methylene chloride and ethyl acetate degrade much more rapidly (over the course of few hours). By far the fastest photodegradation (over the course of few minutes) occurs in chloroform associated with a rapidly increasing green PL.

### 3.1. Degradation Kinetics from Absorption and Emission Spectroscopy

Based on these initial experiments, methylene chloride and ethyl acetate were chosen for further investigation assuming that in these solvents a general representation of the degradation behavior of **L4P** can be achieved in a reasonable duration of UV-irradiation. To get a better understanding of the process of degradation, kinetic studies of three observables were carried out: The absorbance, the blue PL (excited at 330 nm), which is related to native defect-free **L4P**, and the green emission, which is excited below the absorption edge of **L4P** (at 400 nm) for addressing defect-related states directly. As will be detailed below, energy transfer between **L4P** and the defects is an additional process reducing the LOPP's radiative yield. Therefore, in order to elucidate the primary photo-degradation mechanism, the measurements have to be carried out at concentrations sufficiently low to neglect energy transfer. Over the course of irradiation, the narrow absorption peaks around 350 and 370 nm strongly decrease and a broad featureless absorption between 380 and 500 nm rises (**Figure 1**a). In a similar manner the blue **L4P** emission between 370 and 450 nm decreases and loses its vibronic structure (Figure 1c). Simultaneously, a broad green PL appears with a maximum at 480 nm (Figure 1b). The time dependent decrease of both the absorption at the 0–0 transition as well as the blue PL is very similar (Figure 1d), suggesting that these two spectroscopic signatures correspond to one and the same molecular structure, i.e. **L4P**. Interestingly, after the **L4P** is mostly consumed and the maximum concentration of the primary photoproduct is reached, the green emission eventually also starts to decay.

These findings agree somehow with the common photodegradation mechanisms proposed in the literature that involve formation of carbonyl (C = O) group defects, typically at the bridging benzylic sites.[8–10] If photodegradation would therefore follow this kind of mechanism, structures carrying the fluorenone motif, such as **L4P-O** and **L4P-O2** (Scheme 1) should be formed. However, the product mixture of degraded **L4P** in methylene chloride or ethyl acetate displays very different optical spectra as compared to the synthesized ketones **L4P-O** and **L4P-O2** (**Figure 2**). The photodegraded mixtures (Figure 2b) show a broad absorption down to 2.5 eV, signifying the presence of transitions with considerable strength below the absorption edge of **L4P** (3.3 eV, see Figure 1a). This low-energy absorption is still substantial in the region of **L4P** emission, suggesting that energy transfer might be quite efficient, if donor (**L4P**) and acceptor (defect) are in close proximity. The defect emission is bright and at around 2.5 eV. In contrast, the near-UV absorption (3.3–3.9 eV) of the ketones **L4P-O** and **L4P-O2** (Figure 2a) resembles the absorption of **L4P** (Figure 1a), although the extinction coefficient $\varepsilon$ is significantly smaller and the maxima are blue-shifted. Additionally there is a low-energy absorption between 2.5 and 3.3 eV, making these compounds appear orange. Yet this broad transition has a very low oscillator strength such that energy transfer for this type of defects is rather unlikely. Additionally the orange emission of these compounds is farther in the low-energy region than observed for any degradation product or mixture and the emission quantum yield is extremely low. From these data it becomes apparent that both quantum yield of these ketones as well as their spectral overlap with **L4P** is rather low and hence such fluorenone structures are most likely not involved in the observed defect emission.

### 3.2. Chemical Analysis of Photodegradation Products

Another indication arises from comparison with the non-bridged *p*-quarterphenyl **4P**, which should behave very different in case photodamage would occur at the benzylic bridges. However, when analogous degradation experiments were carried out in methylene chloride **4P** behaves similarly to **L4P** (see Supporting Information: Figure S5.2) providing another piece of evidence that the formation of fluorenone defects is rather unlikely to be the main photodegradation process.

ADVANCED FUNCTIONAL MATERIALS
www.afm-journal.de



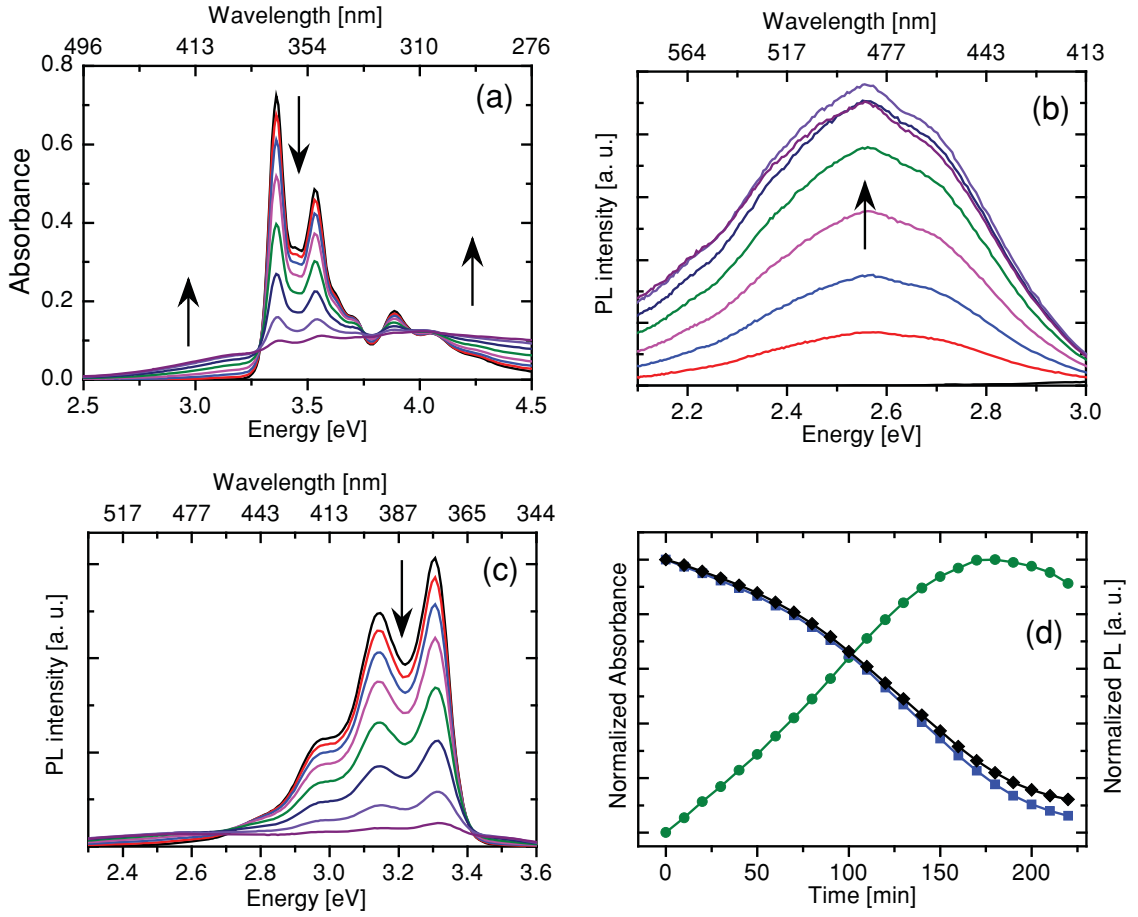


**Figure 1.** Spectral changes upon irradiation of a $6.8 \times 10^{-6}$ mol/L solution of **L4P** in $CH_2Cl_2$ (25 °C) with 300–400 nm light: a) Absorbance spectra, b) corrected photoluminescence (PL) spectra in green region upon 400 nm excitation, and c) corrected PL spectra in blue region upon 330 nm excitation. Spectra shown in a)-c) were recorded every 30 min. d) Resulting plot of changes in absorbance at 369 nm (black diamonds), blue PL detected at 394 nm (blue squares), and green PL detected at 500 nm (green circles) as a function of irradiation time.

In order to elucidate the origin of the defect emission, product formation over time was studied once again in methylene chloride at concentrations compatible with analysis by means of chromatography coupled to mass spectrometry (UPLC-MS). Using UV detection (**Figure 3**b) the main peak at a retention time of 6.86 min is attributed to the starting material **L4P**. Upon irradiation, the first product, which is formed relatively rapidly, exhibits a $m/z$ = 460.2 and a characteristic isotopic pattern, such that it can be assigned to the monochlorinated product **L4P-Cl** (peak at 7.44 min in Figure 3b). Within the proceeding degradation also a relatively large amount of dichlorinated **L4P-$Cl_2$** (see Figures S5.5. and S5.6.) was formed. However, the influence of the chlorination on the optical properties of **L4P** is rather negligible as can be concluded from the transparency at long wavelength. In addition to the singly and doubly chlorinated products, three low-energy absorbing defect-species **L4P-deg** were formed (intense peaks between 6.65 and 6.76 min in Figure 3a, also seen in 3b). All of them show the same $m/z$ = 455.2, which corresponds to a gain of 28 mass units as compared to **L4P**. It turned out to be very difficult to correlate the observed gain in mass with any oxidation process and therefore the chemical nature of the defect cannot be derived from the above analysis. To rule out fragmentation or complex formation upon ionization the ketone **L4P-O** was also analyzed via UPLC-MS, but only a peak at $m/z$ = 413 was found, which corresponds to the [**L4P-O**+H]$^+$-ion. Accordingly, no evidence was found in the photodegraded samples for the presence of the ketones **L4P-O** or **L4P-O2**.

To resolve the chemical structure of the photodegradation products, two of the three main defects **L4P-deg** identified via UPLC-MS monitoring (Figure 3a) were isolated on a scale sufficient for subsequent analysis by NMR spectrocopy (**Figure 4**). Comparison of the $^1$H-NMR spectra of one isomer (**L4P-deg-a**) of the photodegradation products (**L4P-deg**) with **L4P** shows the presence of an additional singlet slightly above 10 ppm, the loss of one proton signal in the aromatic region and the reduced symmetry of the latter. The aliphatic proton signals also indicate a reduction of the molecular symmetry. The corresponding $^{13}$C-NMR spectra may be interpreted the same way and furthermore show the presence of a carbonyl signal. Based on this spectral information, we conclude that upon irradiation of **L4P** in chloroform or methylene chloride a formylation reaction (Figure 4c) occurs, that somewhat resembles the thermal Reimer-Tiemann reaction[16] and gives rise to formation of various monoformylated regioisomers. This would also explain the much more rapid degradation in chloroform as compared to methylene chloride. In the latter, **L4P** primarily undergoes

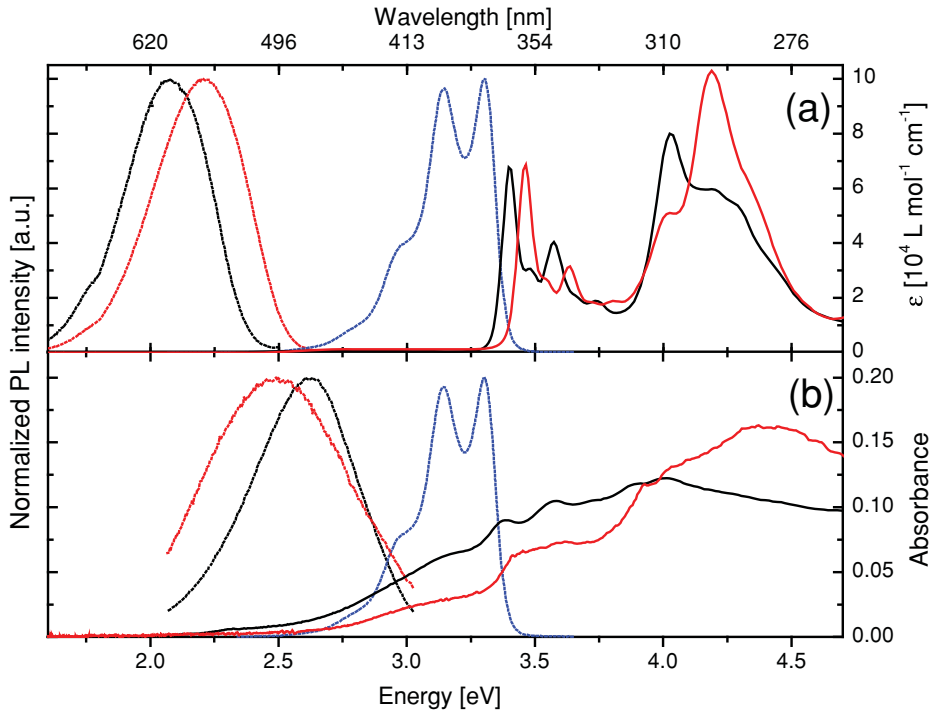


**Figure 2.** a) Absorption spectra of **L4P-O** (solid, black) and **L4P-O2** (solid, red) as well as photoluminescence (PL) spectra of **L4P** (dotted, blue), **L4P-O** (dotted, black), and **L4P-O2** (dotted, red) upon excitation at 330 nm (25 °C, $CH_2Cl_2$). The spectral region between 2.5 and 3.3 eV is not shown because a cutoff filter was used to remove the 2nd harmonic of the excitation source and PL of residual, highly emissive **L4P** in the samples. b) Absorption (solid lines) and PL spectra (dotted lines) of **L4P** after irradiation with 300–400 nm light in $CH_2Cl_2$ (black, initial concentration: $6.8 \times 10^{-6}$ mol/L) and ethyl acetate (red, initial concentration: $6.8 \times 10^{-6}$ mol/L).

chlorination while methylene chloride is being chlorinated itself to in-situ generate chloroform, which is the more reactive formylation agent. Although we can only speculate about the mechanism of this photochemical conversion (potentially involving dichlorocarbenes or precursors of phosgene), it becomes clear now, why especially chloroform, but also methylene chloride, are not suited to process polyfluorenes, polyphenylenes and ladder-type polyphenylenes (since residual solvent is difficult to be removed completely).

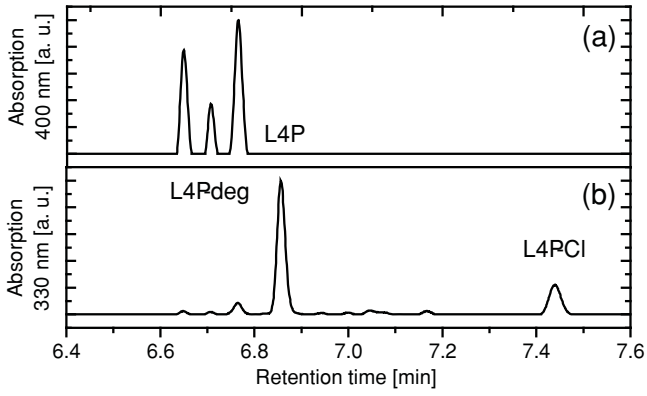


**Figure 3.** Chromatography traces of **L4P** after irradiation with 350 nm light in $CH_2Cl_2$ solution using UV-detection at a) 390–410 nm and b) 325–375 nm giving rise to **L4P-deg** and **L4P-Cl**.

### 3.3. Optical Properties of Isolated Photodegradation Products

Naturally, the spectra of the isolated defects resemble the mixture of photodegraded products (Figure 2b). The absorption spectra of the isolated defects overlap extensively with the emission of **L4P** in the region between 3.0 and 3.5 eV (**Figure 5**a) and, as already mentioned above, energy transfer is expected to occur efficiently. Furthermore the efficiency of the PL of the isolated defects is much higher than that of the ketones **L4P-O** and **L4P-O2** and the emission is situated in the green to yellow region (2.6–2.7 eV). In this context it is interesting to note that careful comparison of the absorption and emission spectra can provide some further insight into the molecular origin of the defects. In the case of **L4P-O** there is a very weak low-energy absorption between 2.3 and 3.2 eV (depicted in Figure 5b in tenfold amplification), which can be attributed to the symmetry-forbidden $n \rightarrow \pi^*$ transition of the ketone. In stark contrast, in **FLO-Ph2**, which has exactly the same $\pi$-system in terms of connectivity, the same transition is significantly stronger, although the $\pi \rightarrow \pi^*$ transition is much weaker. This can readily be explained by the freely rotatable phenyl groups providing more flexibility to the molecule and hence some mixing of the in-plane $\pi \rightarrow \pi^*$ transition and the out-of-plane $n \rightarrow \pi^*$ may occur thereby enhancing the low-energy transition.[17] This influence of backbone rigidity is not only observed in absorption but also in emission: In contrast to **L4P-O**, in **FLO-Ph2** some of the PL is recovered and the quantum yield amounts at least to a few per cent (≈4%) in $CH_2Cl_2$. This implies that the reason for strong low-energy emission of the

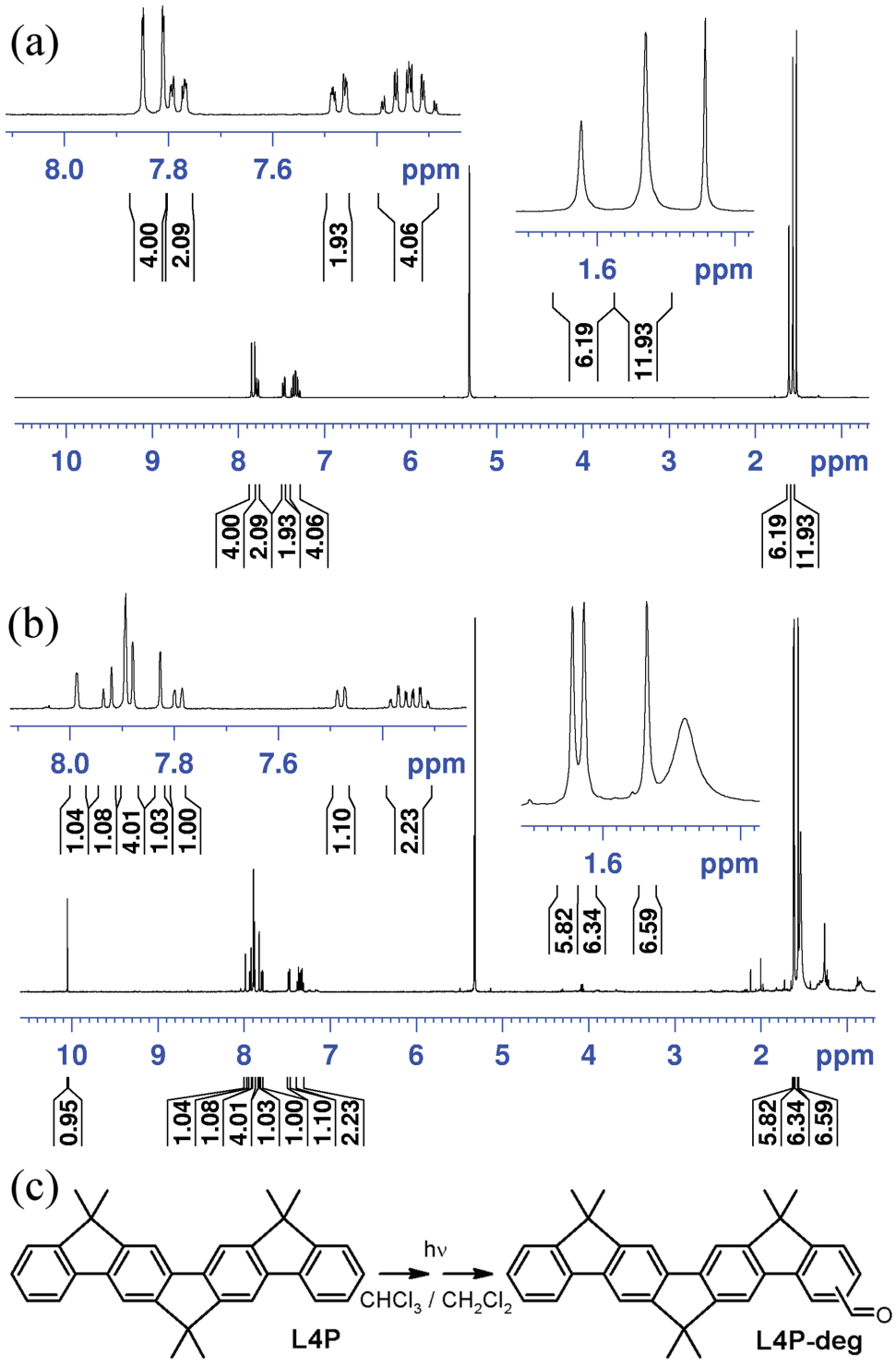


**Figure 4.** Formylation of **L4P** during irradiation in $CH_2Cl_2$ or $CHCl_3$. $^1$H-NMR spectra of a) pristine **L4P** (300 MHz, $CD_2Cl_2$) and b) defect **L4P-deg-a** (500 MHz, $CD_2Cl_2$). c) Proposed photochemical formylation reaction to explain the observed photodegradation products.

isolated photodegradation products is not the broken symmetry due to the reduced planarity of the aromatic system but instead the ability of the carbonyl group to rotate out-of-plane.

Although in chlorinated solvents such as chloroform and methylene chloride we have proven formation of a formylation product, the general validity of these findings and their applicability to explain photodegradation in different solvents or films needed to be investigated. For this purpose, the aging behavior of solutions in methylene chloride and ethyl acetate was compared by means of absorption and PL measurements as well

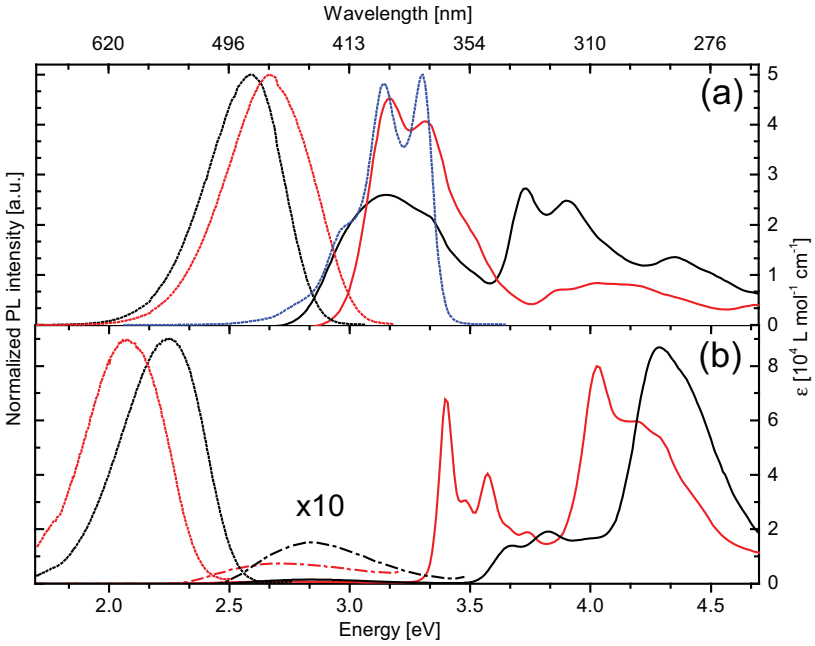


**Figure 5.** a) Absorption (solid lines) and photoluminescence (PL, dotted lines) of two different isolated formyl defects (**L4P-deg** in Figure 4c, excitation at 380 and 395 nm, respectively) and PL of **L4P** (dotted blue, excitation at 330 nm) in $CH_2Cl_2$ (25 °C). b) Absorption (solid and dashed dotted (zoom) lines) and PL spectra (dotted lines) of **L4P-O** (red, excitation at 330 nm) and **FLO-Ph2** (black, excitation at 435 nm) in $CH_2Cl_2$ (25 °C).

as UPLC-MS analysis. In the case of methylene chloride, three main products absorbing around 400 nm were found and are attributed to the three isomers of the formylated product **L4P-deg**. In ethyl acetate there is a large variety of products that absorb above 400 nm, making it—at least by the means that were available for us—not feasible to isolate and characterize them. However, the overall absorption spectra of the irradiated solutions in ethyl acetate (Figure 2b) show qualitatively the same behavior when compared to methylene chloride: Upon irradiation the sharp peaks of the **L4P** absorption are vanishing and a broad tail below 3.3 eV appears, which again overlaps with the **L4P** emission. Even the kinetics of the degradation in ethyl acetate (see Supporting Information: Figure S5.3) is similar to that in methylene chloride.

A very thorough theoretical analysis of the optical properies of potential degradation products of larger oligomers of **LPPP** is given in ref. [7] that discusses three types of defects: a) a "ketonic defect", resembling fluorenone-type defect and hence the structure of **L4P-O**, b) a "phenol defect", and c) a "phenolate defect".[7] While for the first, the calculations of the optical transitions are in good agreement with our findings, the latter two defects arise from the oxidative cleavage of a methylene bridge, resulting in a freely rotatable arylketone fragment adjacent to the phenol unit. Interestingly, in the excited state, these types of structure show allowed transitions below the pristine **LPPP** and in the case of deprotonated species, i.e. the "phenolate defect",[7] the energy of the transition is even below the fluorenone-type defect. In view of our observations and employed experimental conditions as well as the fact that the $\pi$-system of the "phenol defect" somehow resembles **L4P-deg**, which indeed shows low energy emission, even compared to the longer oligomer **L6P**,[11d] it seems most likely that structures related to the "phenol defect"[7] are responsible for the green emission under the conditions employed by us.

Although the products formed in ethyl acetate behave in a very similar manner they are not the same than the ones formed in methylene chloride, as for example proven by their mass spectra. Because typically degradation is referred to an oxidation process in the literature,[4a,7–10] the influence of oxygen on photodegradation was evaluated. Samples of **L4P** in different solvents, each of them under Argon as well as under air, were irradiated at 350 nm at equal conditions. In several solvents (methylene chloride, ethyl acetate, tetrahydrofuran) bubbling Argon through the solution prior to irradiation leads to a significant slow-down of the degradation. The most pronounced difference was found for methylene chloride, where in the Argon-saturated solution the typical **L4P** absorption decreased much more slowly as compared to the aerated sample (**Figure 6**a). Clearly, the absence of oxygen inhibits photodegradation or at least it slows it down (also knowing that water was present in all the samples).

To get another hint towards the oxidation mechanism, different quenchers for active species of oxygen were added to solutions of **L4P** in ethyl acetate prior to

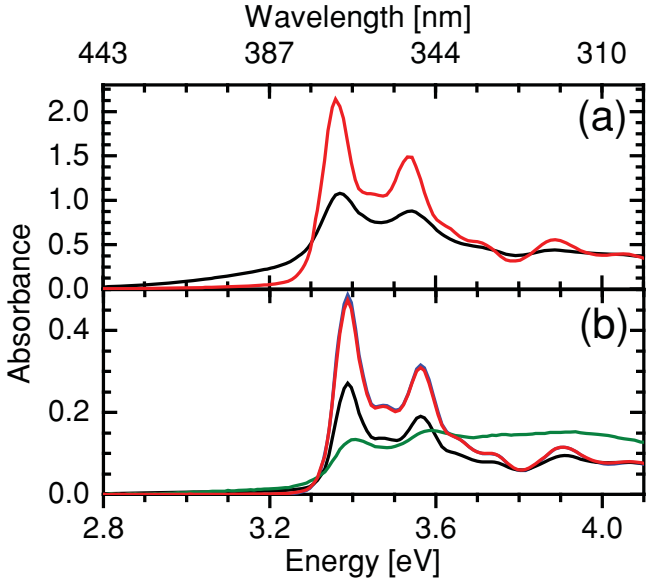


**Figure 6.** a) Absorption (0.2 mm path length) of **L4P** in $CH_2Cl_2$ (initial concentration $10^{-3}$ mol/L) after irradiation with 350 nm light under Argon (red) and under air (black). b) Absorption (1 mm path length) of **L4P** solutions in ethyl acetate (initial concentration $4.4 \times 10^{-5}$ mol/L) after irradiation with 350 nm light in the presence of **DTBP** (green, 0.02 mol/L) or **DABCO** (red, 0.02 mol/L), without an additive (black) as well as the original solution (blue). For solutions containing additives, proper background correction has been carried out (see Supporting Information Figure S5.4 for unprocessed spectra).

irradiation. Namely di-2,6-*tert*-butylphenol (**DTBP**) was added, which is a known scavenger for radical auto-oxidation processes, as well as 1,4-diazabicyclo[2.2.2]octan (**DABCO**), which is a quencher for singlet oxygen.[18] Surprisingly, the addition of **DTBP** did not lead to a longer lifetime of the **L4P** in solution and in contrast the aging even seemed to accelerate (Figure 6b). However, upon addition of **DABCO** practically no photodegradation was observed after the same duration of irradiation. Hence, photodegradation of **L4P** in solution primarily seems to involve singlet oxygen as the main active oxidant. Singlet oxygen engages in variety of reactions, mainly [2+2]- and [4+2]-cycloadditions as well as ene-reactions, involving mostly olefins or dienes, in some cases even aromatic systems, as substrates. Primarily (endo)peroxides and oxetanes are formed in these reactions, which eventually would lead to the formation of ketones and aldehydes.[19] **L4P** does not display one of these particularly priviledged substrate structures giving rise to rather low selectivity during oxidation and the large number of different degradation products obtained in ethyl acetate.

## 4. Degradation in the Solid State and Energy Transfer

While photodegradation of **L4P** is more conveniently studied in dilute solutions, for device applications, such as the hybrid inorganic-organic systems mentioned in the introduction, intermolecular processes, such as crosslinking, exciton migration and excimer formation may have a strong influence.[4d,g,h,k,l,m,p,r,8] Thus it is necessary to work with solid films containing a high concentration of molecules. Therefore, thin layers of **L4P** embedded in a polystyrene (PS) matrix were investigated. Three types of 100 nm thick films (A, B, and C) with increasing **L4P** concentrations of 1, 10, and 20 wt% **L4P**/PS were prepared by spin-casting from toluene solutions onto sapphire substrates. Assuming a homogeneous distribution of the molecules in the matrix, the associated average intermolecular distances decrease from 4 nm over 2 nm to 1.5 nm for samples A, B, and C, respectively. PL spectra of the pristine, unexposed films normalized to **L4P**'s 0–0 transition (**Figure 7**a) are rather similar to the PL spectra in solution (see Figure 1c). However, the high concentration of **L4P** in all films as compared to dilute solutions results in reabsorption of the PL above 3.25 eV, hence the 0–1 transition dominates the emission spectra. Furthermore, a spectrally broad, blue-green emission becomes prominent at increasing concentration. All the experimental data presented below consistently demonstrate that the origin of this emission is the same photochemically generated defect as observed for solutions, while aggregation or excimer formation can be excluded. The defect molecules are already present as impurities in the pristine films and, owing to the much larger molecular concentrations,

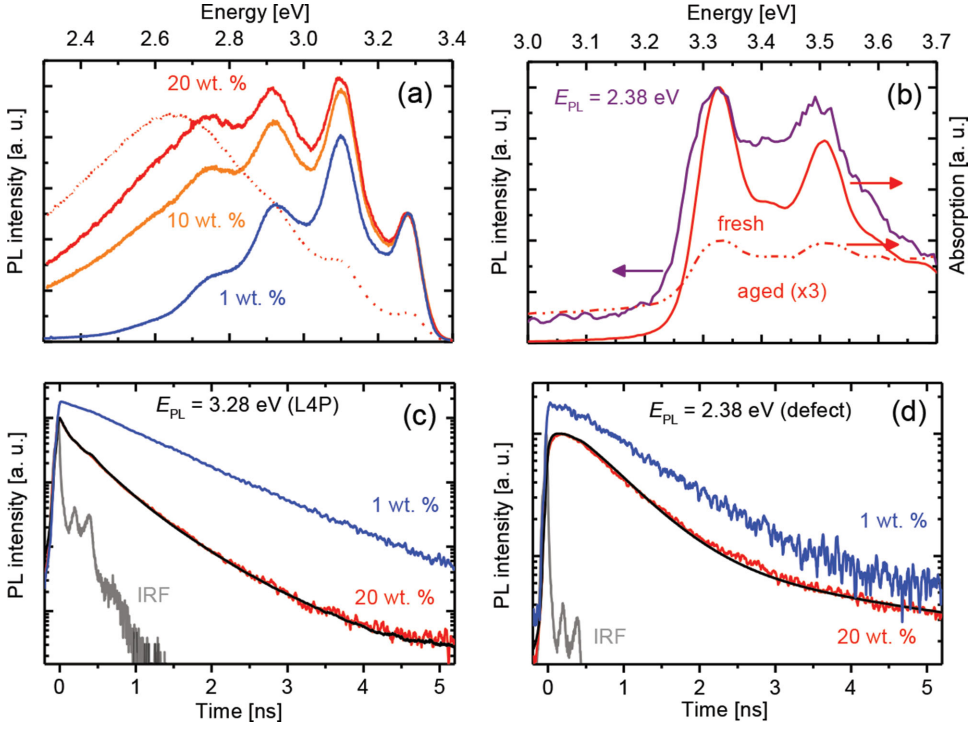


**Figure 7.** Energy transfer from **L4P** to defects in **L4P**/polystyrene (PS) layers on sapphire. a) PL spectra of 100 nm thick pristine films with increasing amount of **L4P**: 1 wt% (blue), 10 wt% (orange), and 20 wt% (red, solid). Spectra are normalized to the 0–0 transition. PL spectrum of the 20 wt% sample after partial photodegradation (red, dash-dotted). b) Absorbance spectra of a pristine (solid, red) and a strongly photo-aged film (dash-dotted, red; spectrum enlarged by a factor of 3 for better visibility) of the 20 wt% sample as well as PL excitation (PLE) spectrum corresponding to the defect emission of a partially photo-aged film (solid, purple; $E_{det}$ = 2.38 eV) of the 20 wt% sample. "Partial" and "strong" aging denotes Ti:Sapphire laser irradiation ($\lambda$ = 350 nm) under ambient conditions for 15 min at 5 W/cm$^2$ and 30 min at 50 W/cm$^2$, respectively. c,d) PL decay of pristine films containing either 1 wt% (blue, shifted for clarity) or 20 wt% (red) of **L4P**. c) PL of **L4P** ($E_{PL}$ = 3.28) and d) defect PL ($E_{PL}$ = 2.38 eV). Black curves are fitting results using a Förster type energy transfer model (for details, see text) convoluted with the instrument response function (IRF, grey lines).

efficient energy transfer occurs here even without extensive photodegradation.

Similarly to solutions (see Figure 1, 6), extended UV irradiation of **L4P**/PS layers leads to a severe reduction of the UV emission and an increase of the blue-green PL component as illustrated exemplarily for a photodegraded layer with 20 wt.% **L4P** (red dash-dotted line in Figure 7a). The increase observed in the low-energy emission upon photodegradation makes it unlikely to originate from aggregates. Addition of **DABCO** to the layer was confirmed to considerably slow down the degradation (see Supporting Information: Figure S4.1). Therefore we assign the process at least in part to singlet-oxygen based photo-oxidation.

The above conclusions are further substantiated by studying the absorption of the layers (Figure 7b). While the absorption of the pristine layer is that of **L4P**, the irradiated film exhibits a reduced and nearly featureless spectrum, which extends to energies below the **L4P** absorption onset at 3.25 eV. Again, this behavior closely resembles that in solution: There, direct excitation of photocreated defects via the low-energy absorption tail is demonstrated (see Figure 1b), leading to the exclusion of excimers as the main source of the blue-green PL. Here, we verify by means of PL excitation (PLE) and time-resolved PL spectroscopy that Förster-type energy transfer from **L4P** to the defects is taking place for sufficiently high concentrations. In PLE, the defect emission at $E_{PL}$ = 2.38 eV of a partially aged layer of type C is monitored as a function of excitation energy. The resulting spectrum (Figure 7b, purple curve) is an envelope to the absorption spectra of the defects and of **L4P**, demonstrating that the defects can be excited either directly or indirectly via the **L4P**.

The dynamics of the ET process was elucidated by time-resolved PL spectroscopy. Pristine layers of type A and C with notably different average intermolecular distances are investigated. In order to avoid effects of photodegradation during the experiment, such as changes in the donor-acceptor ratio,[20] a low excitation density of 0.35 W/cm$^2$ and short integration time of 20 s were chosen. In addition, the samples were kept under vacuum ($10^{-4}$ mbar) inside a cryostat, and each time trace was acquired on a new, previously unexposed sample position. The excited **L4P** and defect populations are monitored at emission energies of 3.28 eV and 2.38 eV, respectively. The decay of the **L4P** emission in layer C (Figure 7c, red line) is markedly non-exponential and much faster than in layer A (Figure 7c, blue line). Thus, an additional decay channel with a time-dependent decay rate has to be present here. Concerning the acceptor dynamics, a rise time is clearly observed in layer C (Figure 7d, red line) but not in layer A (Figure 7d, blue line). This proves the existence of a feeding process to the defect population in the first case.

A Förster-type model[21] that takes into account energy transfer from **L4P** donors to statistically distributed defect acceptors is readily employed to describe the decay dynamics in layer C. Accordingly, the number of excited donors $N_D$ and acceptors $N_A$ follow the rate equations:

$$\dot{N}_D = -k_D N_D - k_T(t) N_D \text{ and } \dot{N}_A = -k_A N_A + k_T(t) N_D \quad (1)$$

Herein, $k_D$ and $k_A$ are the intrinsic donor and acceptor decay rates, respectively, and $k_T(t) = \beta/2\sqrt{k_D/t}$ is the time-dependent energy transfer rate where the prefactor $\beta$ is proportional to the number of unexcited acceptors of density $\rho_A$ within a spherical volume $V$ of Förster radius $R_0$. With the initial conditions $N_D(0) = N_{D,0}$ and $N_A(0) = N_{A,0}$ for a $\delta$-like excitation pulse, the solutions to Equation (1) are given by

$$N_D(t) = N_{D,0} e^{-k_D t} e^{-\beta\sqrt{k_D t}} \text{ and } N_A(t) = N_{A,0} n_A(t) + (k_T N_D * n_A)(t) \quad (2)$$

with $n_A(t) = e^{-k_A t}$ and * being the convolution operator. The acceptor population $N_A(t)$ includes both direct excitation $n_A(t) = e^{-k_A t}$ and excitation via energy transfer $k_T \neq 0$. The model functions (2) are convoluted by the system's instrument response function (Figures 7c and 7d, grey curves) before fitting. As indicated by the black lines in Figures 7c and 7d, both the donor and acceptor decay curves are consistently described by one set of fitting parameters, namely $k_D$ = (1.52 ns)$^{-1}$, $\beta$ = 3.82, $k_A$ = (0.56 ns)$^{-1}$, $\alpha = N_{A,0}/N_{D,0}$ = 0.12. Efficient energy transfer is evidenced by $\beta > 2$ which implies that $k_T(t) > k_D$ up to $t > k_D^{-1}$, that is, energy transfer dominates the total donor decay up to times that are larger than the intrinsic decay time. Being aware of the model's limitations, such as the assumed single exponential intrinsic donor and acceptor decays or the neglect of energy diffusion between donors,[22] the obtained fitting parameters are not discussed in further detail. Finally, it is remarked that the observation of energy transfer from **L4P** molecules to photochemically created defects is not restricted to solid films, but equally applies to highly concentrated solutions (see Supporting Information: Figure S4.3).

## 5. Conclusion

It is demonstrated that small, ladder-type **L4P** molecules dispersed in solution or a solid matrix degrade upon UV irradiation in the presence of oxygen. This photodegradation results in green-yellow emitting defects, which for sufficiently small intermolecular distances are efficiently excited via energy transfer from the original **L4P**. The overall emission process from the defect traps agrees well with previous extensive studies on photodegraded polyfluorene-type polymers.[4c,4k,23]

Considering the process of photodegradation, our system at first appears to be rather similar to what has been proposed for polyfluorenes in the literature (i.e., greenish-yellow emission upon extensive irradiation). But already kinetic studies with **L4P** suggest that neither the fluorenyl anion mechanism,[4a,4f] which should follow typical first order photokinetics, nor the radical chain mechanism[8] may explain our observations. The inhibition of photodegradation by adding **DABCO** to the samples proved, that singlet oxygen is the major source of decomposition, as has already been proposed by Abbel.[10] Thereby, the accelerating kinetics can readily be explained: At the beginning the **L4P** substrate acts as singlet oxygen sensitizer, yet with a rather low sensitization quantum yield.[24] But as soon as the aromatic carbonyl defect has been formed, it acts as a much more efficient singlet oxygen sensitizer due to the enhanced intersystem crossing leading to efficient population of the carbonyl triplet,[25] and hence the photochemical degradation process is auto-catalytic in nature.

At this point it should be emphasized that upon photodegradation no evidence of a derivative of **L4P** carrying the fluorenone motif has been found and that the synthesized ketones **L4P-O** and **L4P-O2** did not exhibit optical properties reminiscent of the actually formed defects in photodegraded **L4P** samples. Our results—in agreement with previous studies[4]—imply that upon photodegradation carbonyl defects are being introduced into the **LPPP** structure; however and more importantly, they suggest that a rigid **LPPP** carrying the fluorenone motif itself cannot explain the typical yellow-to-green defect emission! It appears that the aromatic backbone loses rigidity (as proven in other works)[6,7] by potential cleavage of bridging methylene groups or introduction of rotatable carbonyl groups and therefore symmetry-forbidden $n \rightarrow \pi^*$ transitions become partially allowed as reflected in the corresponding optical spectra. This finding is highly relevant for the critical discussion of reaction mechanisms accounting for the photodegradation in **LPPPs** as well as **PF**, and in organic materials in general.

## Supporting Information

Supporting Information (synthesis and characterization details, description of degradation experiments and time-resolved luminescence spectroscopy) is available from the Wiley Online Library or from the author.

## Acknowledgements

Generous support by the German Research Foundation (DFG via SFB 951) and the Helmholtz Association (via Helmholtz Energy Alliance) is gratefully acknowledged. BASF AG, Bayer Industry Services and Sasol Germany are thanked for generous donations of chemicals.

Received: August 4, 2014
Revised: August 31, 2014
Published online: September 30, 2014

[1] a) *Organic Electronics*, (Ed.: F. So), CRC Press, Boca Raton, FL **2010**; b) *Organic Light Emitting Devices*, (Ed.: K. Müllen, U. Scherf), WILEY-VCH, Weinheim **2006.**

[2] U. Scherf, K. Müllen, *Makromol. Chem. Rapid Commun.* **1991**, *12*, 489.

[3] a) R. H. Friend, R. W. Gymer, A. B. Holmes, J. H. Burroughes, R. N. Marks, C. Taliani, D. D. C. Bradley, D. A. D. Santos, J. L. Brédas, M. Logdlund, W. R. Salaneck, *Nature* **1999**, *397*, 121; b) J. Huber, K. Müllen, J. Salbeck, H. Schenk, U. Scherf, T. Stehlin, R. Stern, *Acta Polymer.* **1994**, *45*, 244.

[4] *For an overview on degradation of polyfluorenes see*: a) U. Scherf, E. J. W. List, *Adv. Mater.* **2002**, *14*, 477; b) S. Gamerith, C. Gadermaier, U. Scherf, E. J. W. List, in *Physics of Organic Semiconductors*, (Ed.:, (Ed.: W. Brütting), WILEY-VCH, Weinheim **2005**, Ch. 6; c) S. Gamerith, C. Gadermaier, U. Scherf, E. J. List, *Phys. Status Solidi* **2004**, *201*, 1132; d) For original research contributions see: d) V. N. Bliznyuk, S. A. Carter, J. C. Scott, G. Klärner, R. D. Miller, D. C. Miller, *Macromolecules* **1999**, *32*, 361; e) E. Zojer, A. Pogantsch, E. Hennebicq, D. Beljonne, J.-L. Brédas, P. S. de Freitas, U. Scherf, E. J. W. List, *J. Chem. Phys.* **2002**, *117*, 6794; f) E. J. W. List, R. Guentner, P. Scandiucci de Freitas, U. Scherf, *Adv. Mater.* **2002**, *14*, 374; g) J. M. Lupton, M. R. Craig, E. W. Meijer, *Appl. Phys. Lett.* **2002**, *80*, 4489; h) S. I. Hintschich, C. Rothe, S. Sinha, A. P. Monkman, P. S. de Freitas, U. Scherf, *J. Chem. Phys.* **2003**, *119*, 12017; i) P. Papadopoulos, G. Floudas, C. Chi, G. Wegner, *J. Chem. Phys.* **2004**, *120*, 2368–2374; k) M. Sims, D. D. C. Bradley, M. Ariu, M. Koeberg, A. Asimakis, M. Grell, D. G. Lidzey, *Adv. Func. Mater.* **2004**, *14*, 765–781; l) C. Gadermaier, L. Romaner, T. Piok, E. J. W. List, B. Souharce, U. Scherf, G. Cerullo, G. Lanzani1, *Phys. Rev. B* **2005**, *72*, 045208; m) C. Chi, C. Im, V. Enkelmann, A. Ziegler, G. Lieser, G. Wegner, *Chem. Eur. J.* **2005**, *11*, 6833–6845; n) K. Becker, J. M. Lupton, J. Feldmann, B. S. Nehls, F. Galbrecht, D. Gao, U. Scherf, *Adv. Funct. Mater.* **2006**, *16*, 364; o) C. Chi, C. Im, G. Wegner, *J. Chem. Phys.* **2006**, *124*, 024907; p) Y.-S. Wu, J. Li, X.-C. Ai, L.-M. Fu, J.-P. Zhang, Y.-Q. Fu, J.-J. Zhou, L. Li, Z.-S. Bo, *J. Phys. Chem. A* **2007**, *111*, 11473; r) J. Kang, J. Jo, Y. Jo, S. Y. Lee, P. E. Keivanidis, G. Wegner, D. Y. Yoon, *Polymer* **2008**, *49*, 5700–5704.

[5] S. Kappaun, H. Scheiber, R. Trattnig, E. Zojer, E. J. W. List, C. Slugovc, *Chem. Commun.* **2008**, 5170–5172.

[6] a) W. Graupner, M. Sacher, M. Graupner, C. Zenz, G. Grampp, A. Hermetter, G. Leising in *Electrical, Optical, and Magnetic Properties of Organic Solid-State Materials IV*, (Ed.: J. R. Reynolds, A. K.-Y. Jen, M. F. Rubner, L. Y. Chiang, L. R. Dalton), Materials Research Society, Warrendale, PA **1998**, 789; b) E. J. W. List, J. Partee, J. Shinar, U. Scherf, K. Müllen, E. Zojer, K. Petritsch, G. Leising, W. Graupner, *Phys. Rev. B* **2000**, *61*, 10807; c) L. Liu, S. Qiu, B. Wang, W. Zhang, P. Lu, Z. Xie, M. Hanif, Y. Ma, J. Shen, *J. Phys. Chem. B* **2005**, *109*, 23366.

[7] L. Romaner, G. Heimel, H. Wiesenhofer, P. Scandiucci de Freitas, U. Scherf, J.-L. Brédas, E. Zojer, E. J. W. List, *Chem. Mater.* **2004**, *16*, 4667–4674.

[8] a) B. W. Zhao, T. Cao, J. M. White, *Adv. Funct. Mater.* **2004**, *14*, 783; b) R. Grisorio, G. P. Suranna, P. Mastrorilli, C. F. Nobile, *Adv. Funct. Mater.* **2007**, *17*, 538.

[9] a) L. Liu, S. Tang, M. Liu, Z. Xie, W. Zhang, P. Lu, M. Hanif, Y. Ma, *J. Phys. Chem. B* **2006**, *110*, 13734; b) R. Grisorio, G. Allegretta, P. Mastrorilli, G. P. Suranna, *Macromolecules* **2011**, *44*, 7977.

[10] R. Abbel, M. Wolffs, R. A. A. Bovee, J. L. J. van Dongen, X. Lou, O. Henze, W. J. Feast, E. W. Meijer, A. P. H. J. Schenning, *Adv. Mater.* **2009**, *21*, 597.

[11] a) V. M. Agranovich, Y. N. Gartstein, M. Litinskaya, *Chem. Rev.* **2011**, *111*, 5179; b) S. Blumstengel, S. Sadofev, C. Xu, J. Puls, R. L. Johnson, H. Glowatzki, N. Koch, F. Henneberger, *Pys. Rev. B* **2008**, *77*, 085323; c) S. Blumstengel, H. Glowatzki, S. Sadofev, N. Koch, S. Kowarik, J. P. Rabe, F. Henneberger, *Phys. Chem. Chem. Phys.* **2010**, *12*, 11642; d) B. Kobin, L. Grubert, S. Blumstengel, F. Henneberger, S. Hecht, *J. Mater. Chem.* **2012**, *22*, 4383.

[12] L4P,as well as **L4P-O2** have been described in M. Kimura (Idemitsu Kosan Co., Ltd.), *EP 1860 097 A1*, **2007**; however the synthetic route involves harsh conditions, characterization data for the "intermediates" was not provided, and some of the few properties given are obviously different in reality.

[13] G. Goldschmiedt, F. Schranzhofer, *Monatshefte für Chemie* **1895**, *16*, 807.

[14] B. A. Haag, C. Sämann, A. Jana, P. Knochel, *Angew. Chem. Int. Ed.* **2011**, *50*, 7290; *Angew. Chem.* **2011**, *123*, 7428.

[15] *The procedure was adapted from*: J. H. Markgraf, B. Y. Choi, *Synth. Commun.* **1999**, *29*, 2405.

[16] a) K. Reimer, F. Tiemann, *Chem. Ber.* **1876**, *9*, 824; b) L. Kürti, B. Czakó, *Strategic Applications of Named Reactions in Organic Synthesis*, Elsevier, Burlington, San Diego, London **2005**, 378.

[17] N. J. Turro, V. Ramamurthy, J. C. Scaiano, *Modern Molecular Photochemistry of Organic Molecules*, University Science Books, Sausalito, CA **2010**, Sec. 4 23–4.26.

[18] A. G. Griesbeck, T. T. El-Idreesy, W. Adam, O. Krebs in *CRC Handbook of Organic Photochemistry and Photobiology*, 2nd Ed, (Eds. W. Horspool, F. Lenci), CRC Press Boca Raton, FL **2004**, Ch. 8.

[19] a) C. S. Foote, *Acc. Chem. Res.* **1968**, *1*, 104–110; b) W. Ando, S. Kohmoto, *Chem. Commun.* **1978**, 120–121; c) *CRC*

*Handbook of Organic Photochemistry and Photobiology*, **2nd Ed**, (Eds: W. Horspool, F. Lenci), CRC Press, Boca Raton, FL **2004**, Ch. 4, 8, 25, 45, 108.

[20] That photodegradation is indeed influencing the ET dynamics by increasing the acceptor-donor ratio is demonstrated in Figure S4.2 of the supporting information.

[21] Th. Förster, *Z. Naturforsch.* **1949**, *4a*, 321.

[22] E. Engel, K. Leo, M. Hoffmann, *Chem. Phys.* **2006**, *325*, 170.

[23] H. Marciniak, M. Teicher, U. Scherf, S. Trost, T. Riedl, M. Lehnhardt, T. Rabe, W. Kowalksy, S. Lochbrunner, *Phys. Rev. B* **2012**, *85*, 214204.

[24] S. M. Fonseca, J. Pina, L. G. Arnaut, J. Seixas de Melo, H. D. Burrows, N. Chattopadhyay, L. Alcácer, A. Charas, J. Morgado, A. P. Monkman, U. Asawapirom, U. Scherf, R. Edge, S. Navaratnam, *J. Phys. Chem. B* **2006**, *110*, 8278.

[25] N. J. Turro, V. Ramamurthy, J. C. Scaiano, *Modern Molecular Photochemistry of Organic Molecules*, University Science Books, Sausalito, CA **2010**, Sec. 14.6.